

California Fruit Tree, Nut Tree and Grapevine Improvement Advisory Board (IAB)



2020 Research Progress Report

Nursery Services Program
California Department of Food and Agriculture
Sacramento, CA 95814

TABLE OF CONTENTS

Reports

- I. Almond Bud Failure Genetic Disorder
Thomas Gradzie..... Pages 1-11
- II. Study of the Effects of Little cherry virus-1 and Little cherry virus-2 on Different Cherry Rootstocks*
Maher Al Rwahnih Pages 12-16
- III. Development and validation of real-time quantitative PCR assays for the detection of fruit tree viruses
Maher Al Rwahnih..... Pages 17-26
- IV. Improved Detection and Evaluation of the Biological Significance of Grapevine Vitiviruses
Maher Al Rwahnih..... Pages 27-31
- V. Managing Fungal Trunk Diseases in Plant Nursery Stock
Philippe Rolshausen..... Pages 32-36
- VI. The Development of an Armillaria Resistance Screen for Clonal Walnut Rootstock
Pat J. Brown..... In Progress
- VII. Support Foundation Plan 2019/ 2020
In Progress...
- VIII. Breeding and Selection of Apple Rootstocks to Match California Industry Needs
Genarro Fazio..... In Progress
- IX. Design and delivery of protein chimeras for therapy of viral diseases in grape
Miller..... In Progress

X. Evaluating novel nematicidal chemistry for usefulness in the nursery industry
Andreas Westphal..... In Progress

**Progress report on a research grant proposal to: Fruit Tree, Nut Tree and Grapevine
Improvement Advisory Board (IAB)**

Project Title: **Almond Bud Failure Genetic Disorder** (Year 2 of 2)

Project Leader: Tom Gradziel

Cooperating Personnel: Jonathan Fresnedo Ramirez, Katherine D'Amico-Willman, (Ohio State.), William Hazard, and Megan Lynch.

Location: Department of Plant Sciences, Univ. of California at Davis

Summary.

The failure or significant delay of vegetative bud development and growth weakens tree productivity in the current year through the decreased availability of new shoots and leaves for photosynthesis and in the following years through decreased flower-bearing wood and so potential yields. Bud 'pushing' failures have a range of possible causes, including virus and bacterial infections, nutrient deficiencies and weak winter vernalization (10). Genetic bud-failures are those associated with specific genotypes (varieties) including Noninfectious Bud Failure (NBF) in Nonpareil, Carmel and others, and Environmental Bud Failure (EBF) in Monterey and others. NBF and EBF both result in bud-failures but differ in their induction, developmental-timelines and ultimate cause of collapse. Understanding these differences is important for both diagnosis and management.

Genetic control of **Noninfectious Bud Failure** has been demonstrated in crossing studies with almond and peach (10, 14). Noninfectious bud-failure does not result from a genetic change but rather a change in the state of a hypothetical 'dormancy' gene; in effect, this gene is turned-off at the wrong time and this change is irreversible once a certain genetic 'age' is achieved (1, 8, 14). Results from 2020 summer dormant bud-pushing studies support our preliminary hypothesis that this gene also functions in a hypothesized summer dormancy in almond, and this is when initial induction/triggering of the disorder may occur. [A critical diagnostic for NBF is that vegetative buds are already dead (necrotic and brown at the core) going into winter dormancy in the fall, further indicating that the induction occurred during a previous growing season]. Mechanisms for controlling gene action without changing gene identity are known as epigenetic mechanisms and include changes in gene methylation (11, 12), chromosome (telomere) structure (13), micro-RNA composition as well as several still poorly understood processes (2). Results from the Almond Board of California (ABC) funded collaborative OSU studies also support earlier findings (8) that methylation changes are associated (whether causative or not) with the NBF genetic-aging, and so can be used for more accurate diagnostics as well as better management. Recent OSU research collaborations have identified methylation events in propagation sources that are strongly associated with (and so possible predictors of) high probability of NBF expression in trees propagated from those sources (11, 12). In addition, we are pursuing more general and so more readily diagnosed methylation patterns associated with general aging that could then be directly used to better manage aging in FPS clones of Carmel and possibly Nonpareil, and so indirectly suppress their advancement to NBF expression. [FPS foundation trees are heavily pruned to selectively push dormant (and so reduced age)

epicormic buds rather than axillary shoot buds where genetic ageing continues to advance in resulting propagation wood (1, 9). However, with the current intensity of FPS pruning it is often difficult to determine whether the bud pushed is a true epicormic bud rather than a more basal axillary shoot bud. Molecular markers based on general methylation status (2, 8, 11, 12) should be able to rapidly discriminate these two types of buds with eventual marker deployment similar to molecular fingerprinting/virus-screening currently routinely employed at FPS]. We continue to screen for such useful methylation markers and to further verify the origins (current season axillary or dormant epicormic bud) through tissue-sectioning to identify vascular trace and so differentiate bud development patterns and timelines. This plant tissue analysis could also help us identify the tissue where NBF is initially triggered (leaf, bark, bud, etc.) for screening useful molecular markers. Somewhat disturbingly, data analysis completed in 2020/21 concludes that the induction and subsequent development of NBF does not follow the fairly well-characterized sectoring patterns usually seen in horticultural budspouts (6) but rather the entire shoot tissue is uniformly altered. Consequently, the site of the putative (methylation, etc.) triggering of NBF may occur in tissue outside the shoot or much earlier in shoot meristem development, suggesting that using leaf samples from affected shoots may not be the best strategy to isolating the genetic/epigenetic trigger.

In contrast, the greater site, source and year-to-year variability in **Environmental Bud Failure** (EBF) suggests that while it is associated with certain highly susceptible genotypes (varieties) it is strongly affected/triggered by environmental factors such as diseases and/or other stresses during the previous growing season and climate conditions during dormancy. Environmental bud-failure is activated at some time between fall dormancy and bud-pushing the following spring, but the specific time (and so mechanism) of failure has not been determined partly because of a lack of useful developmental milestones for bud development during dormancy. Research in 2020 and 2021 has shown that the number of leaf primordia in dormant Nonpareil as well as Monterey buds continue to show a fairly uniform rate of increase throughout dormancy and that this internal bud-growth pattern can be used to establish a developmental timeline for normal dormant bud development as well as providing more specific estimates for the time of EBF bud collapse. As in 2020, the increase in number of 2021 leaf primordia was relatively uniform among and between varieties and among shoots from different parts of the trees early in the dormant season. Variability among shoots for both varieties tested dramatically increased in February, 2021 but not 2022. Our initial interpretation was that by this time in 2021, chilling requirements were satisfied, and further growth became dependent on available heat units as well as nutrient reserves within individual buds. Because heat units would be relatively uniform throughout the tree, nutrient availability would be the most likely cause of the large differences seen in subsequent bud development observed in 2020/21. These 2020/21 findings are consistent with the hypothesis that EBF susceptible varieties such as Monterey are more vulnerable to nutrient depletion during late dormancy. Depletion of crucial nutrients such as carbohydrate reserves would be dependent on levels of reserves going into dormancy (which would be reduced in stressed trees) as well as heat -dependent rate of carbohydrate loss (which would be increased in warmer January-February temperatures). However, this hypothesis would predict that the unusually high spring temperatures in 2022 would have resulted in more and earlier carbohydrate depletion resulting in a greater numbers of stalled bud development and so a greater variability in the amount of final bud-push observed. However, increased variability among spring, 2022 buds was not observed, indicating that the carbohydrate depletion model may be incomplete.

While it is expected that the deeper dormancy of epicormic buds would show different and much reduced leaf primordia development patterns, the status of these epicormic buds is still critical to grower/nursery tree management decisions when EBF occurs (particularly on young trees) because it will provide important information in determining whether the sporadic incidents of EBF can be effectively managed by pruning-back affected shoots to push any available epicormic shoots (waterspouts).

Objectives.

- A. Identify effective developmental timelines for vegetative bud induction and progression through dormancy.

Identifying accurate developmental timelines is required to validate NBF as well as EBF models and provide genetic, epigenetic, and physiological targets for remediation as well as biomarker reference points for vegetative-bud development including stage of failure.

- B. Characterize the origin, structure and development pattern of epicormic meristems.

Differentiating the origin, structure and dormancy patterns of epicormic relative to axillary meristems will improve our understanding of latent-bud status/inducibility and will facilitate grower 'maintain vs. replant' decisions when faced with severe vernalization-failure induced blind-wood. Such improved understanding is also critical to maintaining low Noninfectious Bud-failure sources of FPS foundation nursery stock.

- C. Identify molecular and/or biochemical markers for identifying sources with increased risk of bud-failure.

Mapping methylation changes in vegetative-buds during early development provides reference points for comparison against subsequent failure in both NFB and EBF. These molecular-based reference points can then be used to synchronize and interpret ongoing ABC funded projects such as the Z-lab bud-carbohydrate study as well as a SCRI-type vernalization (chilling/heat requirement responses to climate change) project currently being developed.

Results (2-years)

Summer dormancy in (dryland) almond. In 2021, the degree of summer-dormancy for commercially grown Nonpareil compared against traditional dryland/almond-rooted Nonpareil, was characterized by pruning back terminal shoot growth at various times during the summer (Fig. 1) in order to induce growth in more basal axillary buds. The proportion of axillary buds subsequently pushing new growth during the different times of summer were used as an estimate of the level of summer dormancy within trees at these times. Results document a high level of mid-to-late summer-dormancy under dryland conditions but much less so under commercial practices. Both tests showed a significant uptick in axillary bud pushing success in early July, though this may be the result of a local weather event

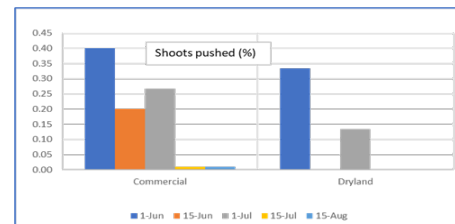


Fig. 1. The proportion of axillary buds induced to push by apical (shoot growing tip) pruning.

because the plots were within a mile of each other. The failure to achieve sufficient summer-dormancy may be the trigger (according to the Kester model) that accelerates the expression of NBF under the highly intensive commercial growth conditions in California. Our results support this model and also demonstrate that almond has the inherent capacity to suppress mid to late summer vegetative growth which might be exploited to divert more available irrigation water to yield rather than excessive vegetative growth.

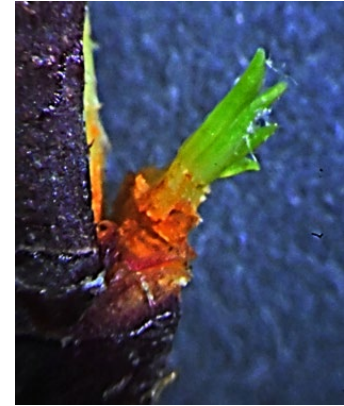


Fig. 2. Leaf primordia visible in dissected 2021 axillary bud in mid-December showing very similar structure to that observed in 2020.

A. Identify effective developmental timelines. Several possible markers for stage of dormant bud development were evaluated in 2020/21 including bud size, bud-scale characteristics, and the number of leaf primordia visible using a dissecting microscope. The number of leaf primordia was chosen for more extensive study due to its relatively straightforward characterization (Fig. 2) and relatively consistent and easily discernible change over time during the dormant season (Fig. 3). Plots of results over time from both 2020 as well as 2021 show that the number of leaf primordia in dormant Nonpareil as well as Monterey buds show a fairly uniform increase throughout dormancy and that this internal growth pattern can be used to establish a developmental timeline for normal dormant-bud development as well as providing more precise estimates for the time of any bud collapse within this period. Interestingly, while number of leaf primordia showed a relatively uniform increase for both varieties as well as among shoots from different parts of the trees early in the dormant season, in 2021 differences among shoots for both varieties dramatically increased in February which is shown by the large increased variation for the individual leaf primordia counts (the sample standard deviation is plotted as vertical lines for each evaluation date). Our initial interpretation was that by this time chilling requirements were satisfied, and further growth became dependent on available heat units as well as available nutrient reserves within individual buds. Because heat units were relatively uniform throughout the tree, differences in nutrient availability would be the most likely cause of the large differences seen in subsequent leaf primordia development. These findings are consistent with the hypothesis that in EBF susceptible varieties such as Monterey are more vulnerable to nutrient depletion during late dormancy. Depletion of crucial nutrients such as carbohydrate reserves would be dependent on levels of reserves available going into dormancy (which would be reduced in stressed trees) as well as heat-dependent rate of carbohydrate depletion (which would be increased in warmer January-February temperatures). However, this hypothesis predicted that the exceptionally high spring temperatures in spring, 2022 would contribute to more and earlier carbohydrate depletion (2021/22 bud development appeared to be about 2-weeks ahead of 2020/21) resulting in a greater numbers of stalled bud development and so an even greater variability in the final numbers of leaf primordia observed. In fact, a reduced variability among

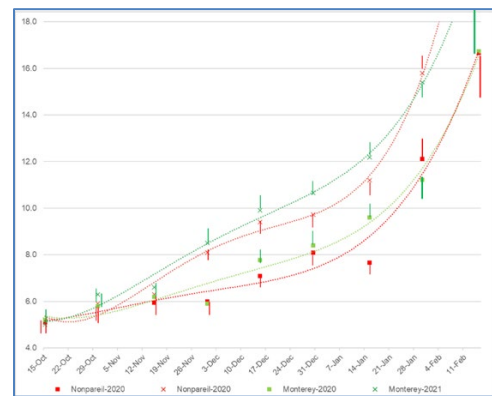


Fig. 3. Average number of leaf primordia visible in dissected axillary buds at different times of the winter dormant period. (Sample standard deviation shown as vertical lines).

2022 buds was actually observed, indicating that the carbohydrate depletion model may be too simplistic.

Axillary vegetative bud dissections in 2021/2022 also identified an increase in bud development aberrations, specifically the ectopic or out-of-place development of budscale-like primordia. Dormant vegetative buds are surrounded and protected by brown, woody budscales (see Fig. 7) which are the developmental equivalent of modified leaf primordia (Fig. 4). Budscales are fully formed by the time vegetative buds go into fall dormancy. (In fact, the development of dark brown pubescence on fall budscales is often used as an indicator of the transition to full dormancy). Buds will show a transition from a spade-shaped scale to more clearly defined leaf primordia in dissections at this time. In spring, 2022, however, we detected a greater number of budscale-like primordia located well within later stages of leaf primordia. While these ectopic budscale primordia appeared to cause some disorganization of normal leaf phyllotaxy, the effect, if any, on bud viability remains unknown.



Fig. 4. Typical late-stage leaf primordia showing basal stipules (left) note the distinct leaf veins and feathery outer edges. Adjacent ectopic budscale showing smooth edges with some early lignification and browning occurring at the tip (right).

B. Characterize the origin, structure and development pattern of epicormic meristems.



Fig. 5. FPS Carmel source-clone tree maintained by intensive annual hedging.

Differentiating the origin, structure and dormancy patterns of epicormic relative to axillary meristems remains crucial to the maintenance of FPS foundation source-clones retaining low probability of NBF expression in subsequent vegetative progeny trees (Figs. 5 and 7). Accurate knowledge of epicormic bud viability is also required for growers/nurseries faced with extensive blind wood associated with EBF (Fig. 6) because the presence of viable epicormic buds provides a strategy for rebuilding tree architecture through intensive pruning to push these otherwise dormant buds. This can be particularly important in grower ‘maintain vs. replant’ decisions when faced with severe EBF induced blindwood as



Fig. 6. Blind wood on EBF affected Monterey showing the effect of pushing of epicormic buds forming water-sprout shoots

occurred in 2020. Figs. 5 & 7 show new shoot growth in FPS foundation Carmel trees after extensive dormant season pruning. Ideally, the FPS goal would be to push mainly dormant epicormic buds because the potential for expressing NBF increases with the sequential generations of terminal shoot leafout and development. In Fig. 7 (left) the small arrow identifies two shoots growing from basal axillary buds of the previous season's shoot (as determined by subsequent sectioning the shoots and following the characteristic vascular pattern to the shoot xylem). In contrast, the lateral meristems associated with epicormic buds (one

identified by long arrow) are true epicormic meristems with inherently lower potential for conveying NBF. We are continuing to examine different morphological (via tissue dissection) and molecular (described below) approaches to allow more rapid and accurate discrimination of these buds in the field. (In contrast to normal preformed axillary buds where vascular strands follow the phyllotaxis spiral, epicormic vascular connections appear to be associated with vascular strands possibly from lateral bud scales in dormant buds (Fig. 7-right).

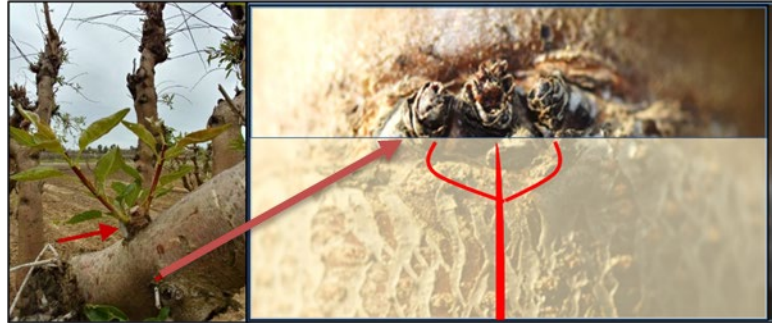


Fig. 7. The pushing of basal axillary shoots (left) adjacent to dormant epicormic meristems (right) in in FPS Carmel source-clone. [Right-inset, the pattern of internal vascular development for the 4-year-old central axillary bud showing proximal branching feeding the 2 lateral epicormic buds in a pattern distinctly different from the spiral connections associated with adjacent axillary buds].

Our previous working model for epicormic bud origin was mainly based on cross sections of 4 year and older branches where the recently emerged epicormic bud position could be tracked back to remnant vascular "traces" originating relatively early in the branch development. In this scenario, epigenetic aging was suppressed because the vascular traces remained meristematic without forming the structured meristems or vegetative buds where aging is presumed to occur. Extensive bud sectioning in 2021 suggests a new model where axillary buds in older branch would represent buds maintained from the original one-year-old shoot but which have maintained their existence by the production of one to 2 leaves per year for the small (2-4 millimeter) continuation of growth required to maintain a viable (though highly suppressed) meristem for the subsequent year. Natural branch breakage or artificial pruning would push this bud into active growth. Alternatively, if it failed to produce sufficient leaves for the photosynthesis needed for continued existence, it would die as shown in Fig. 7-right. However, in almond and closely related species such as peach these older buds will also form 2 adjacent, primal meristems which are the epicormic meristems. When the central axillary meristems dies, it releases one or both of the lateral epicormic meristems to begin growth, often being very suppressed growth because of its location in older and shaded wood where it would become in essence structurally equivalent to the parent axillary bud with a developed but poorly formed meristem structure as well as the need to continue some minimal growth to maintain its continued existence. This equivalence to the axillary bud also includes the formation of its own lateral epicormic meristems. A schematic example of this repeated pattern of punctuated Epicormic transitions is shown in Fig. 9. Because the distance between the central axillary bud and lateral epicormic buds is typically only a few millimeters, tracing the vascular development feeding these transitions would look highly continuous, such as that shown



Fig. 8. Brands cross-section following the continuous trace from recently emerging epicormic meristem to central pit region.

in Fig. 8 [If, however, the branch becomes broken, either through wind damage or artificial pruning, epicormic meristems can be released and will grow very aggressive watersprouts type shoots because of the wealth of newly available nutrients and sunlight that the pruning has provided and because the lack of a well-structured meristem in the epicormics results in shoots growing indefinitely as long as nutrients and proper environment is available (rather than the usual growth slow-down and even arrest associated with normal axillary meristems once the original bud has grown (i.e. expanded largely by internode extension of its typically 25-30 preformed nodes). This latter hypothesis of punctuated transitions is consistent with field observations for almond but is inconsistent with our hypothesis that epicormics remain relatively ageless because they fail to form structured meristems (but rather are maintained as meristematic vascular traces as proposed in Fig. 7). In our new hypothesis (Fig. 9), based largely on 2021 branch bud dissections, epicormic buds are spun off originally from an axillary bud and then subsequently through sequential transition to lateral epicormic buds (that form normal axillary type structured meristems along with their own lateral meristems-which again will continue the potential for shoot growth if the new axillary-type meristem dies off). Consequently, the epicormic lineages are maintained by a series of structured (though suppressed) meristems,-bringing us back to the problem of how these lineages avoid epigenetic aging.

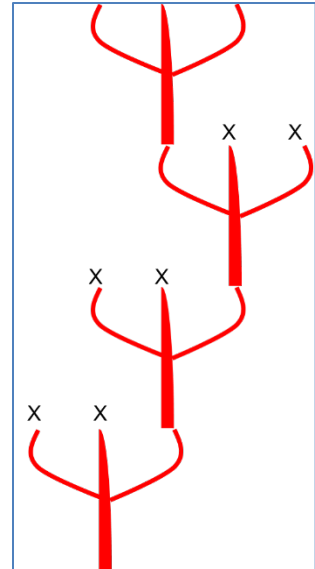


Fig. 9. The repeated pattern of punctuated epicormic transitions. (X - meristem death). Multiple years of incremental growth commonly occur between transitions.

To make matters more confusing, we have recently identified a closely related species, *Prunus mira* or the Tibetan peach which appears to be able to form adventitious shoots from the remnant traces of both leaf, bud and possibly budscales (Fig. 10), thereby supporting our original hypothesis. We have recently made crosses between Tibetan peach and the commercial peach (*Prunus persica*) which forms epicormic nodes very similar to that of almond. The pattern of epicormic development in their progeny may help us understand their origin and mechanism of epicormic maintenance/propagation.

C. Identify molecular and/or biochemical markers. Results from 2020 and 2021 collaborative OSU studies continue to support earlier findings (8) that some methylation changes are associated with NBF genetic-aging, and so might be used for more accurate diagnostics as well as improved management. A significant problem is that almond possesses a huge amount of methylation variability within each of its 8 chromosomes. (Fig. 11). The challenge continues to be sorting out which of these are functionally related to NBF expression and which seem associated only by chance due to the tens of thousands of potential markers being analyzed (see citations 11 and



Fig. 10. Proliferation of meristems and subsequent shoots from the axillary meristems and in adjacent epicormic meristem (now dead) as well as the 3 vascular traces of the detached leaf (lower 3 shoots) in the wild peach species *P. mira*.

12). We are continuing OSU research collaborations in Almond Board of California funded projects to identify specific methylation markers in FPS propagation sources that are strongly associated with (and so good predictors of) high probability of NBF expression in trees propagated from those sources. In a separate project, we are pursuing more general and so more readily diagnosed methylation patterns associated with general clone-aging that could then be indirectly used to better manage clone-aging in specific FPS clones of Nonpareil and Carmel, and so indirectly suppress their advancement to inevitable NBF expression. FPS foundation trees are routinely heavily pruned with the goal to selectively push dormant (and so reduced-age) epicormic buds rather than axillary shoot buds (where genetic ageing continues to advance in resulting propagation wood) (1, 9). However, as discussed above, with the current intensity of FPS pruning it is often difficult to determine whether the bud pushed is a true epicormic bud rather than a more basal axillary shoot bud. Molecular markers based on general methylation status (2, 8, 11, 12) might be able to more rapidly discriminate these two types of buds. If we could identify age related methylation markers that consistently change with shoot age in the specific FPS low-NBF Carmel clonal source, this could prove very useful for developing pruning and shoot epigenotyping methods to more precisely select low NBF propagation wood. For example, Fig. 5 shows the FPS Carmel source clone. Identifying a specific methylation marker which discriminates terminal shoot types from low-clonal-age shoot types such as the epicormic shoots originating near the base of the tree, might then allow rapid discrimination of shoot-type without the need for tissue dissections. An advantage of this marker-based system is that it is very similar to molecular fingerprinting/virus-screening currently routinely employed at FPS. However, it may prove to be effective only for this Carmel foundation source, but even this limited applicability would be valuable since there is currently only one FPS foundation source for Carmel. We also continue to pursue morphological markers to discriminate basal axillary versus true epicormic buds through tissue-sectioning to differentiate their vascular trace patterns (as in Fig. 7). This plant tissue analysis could also help identify the best target tissue (leaf, bark, bud, etc.) for ultimately identifying the specific site of molecular triggers for NBF expression. Somewhat disturbingly, data analysis completed in 2020 concludes that the induction and subsequent development of NBF does not follow the well-characterized sectoring patterns usually seen in horticultural budsports (6) but rather the entire shoot tissue is uniformly altered. In typical budsports, the mutation has occurred in shoot apical meristem (SAM) cells where subsequent divisions produce plant tissues in which altered expression and development can be recognized and studied within the resultant shoot sector.

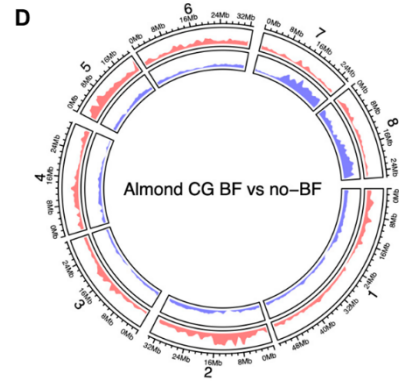


Fig. 11. Summary of CG-methylation patterns over each of the 8 almond chromosomes for a clone with NBF compared with trees of the same clone but showing no NBF.

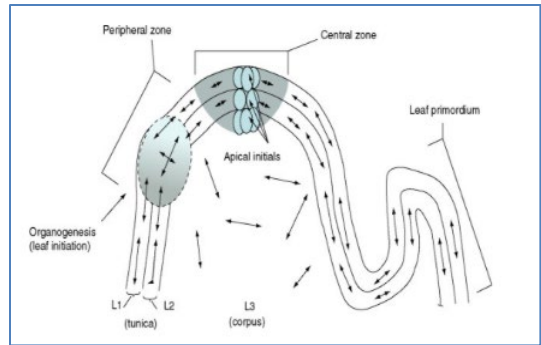


Fig 12. Shoot apical meristems of most angiosperms consists of one to several distinct layers of tunica, where cells divide anticlinally, and of the inner corpus, with cells dividing both anticlinally and periclinally. Multiple initial cells contribute to these different layers.

Because shoot apical meristems in plants occurs within a tunica-carpus structure with multiple cell initials (Fig. 12), any mutations initiated in the meristem would be transmitted to daughter cells and subsequent tissues as unique sectors (Fig. 13). In the expected sectorial chimera, such as those shown in Fig. 13, the mutated sector would be expected to show high NBF while axillary buds from the rest of that shoot would be free of NBF in individual trees propagated from that bud. This should result in a high variability in NBF response within individual shoots, ranging from high NBF expression to none. However, long-term field results plotted in Fig. 14 show that essentially all axillary buds from any given shoot will show very similar NBF responses in subsequently propagated trees. Consequently, the site of the putative mutation event (methylation, etc.) triggering NBF may occur in tissue outside the shoot, suggesting that using leaf samples from affected shoots may not be an effective sampling site for isolating the putative genetic/epigenetic trigger as it may be occurring elsewhere. If verified, the unorthodox nature of this findings would suggest that we may have to rethink traditional mechanisms and testing approaches to successfully identify the actual triggering mechanism.

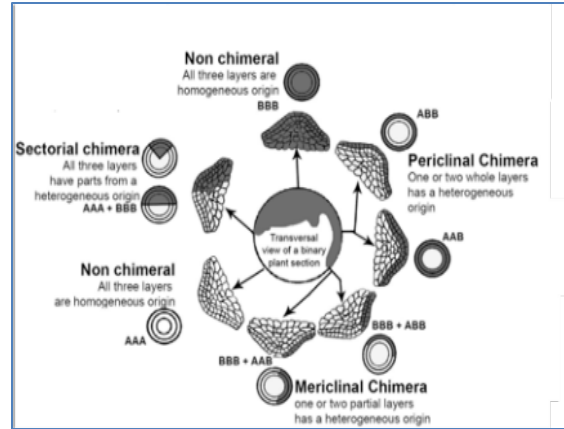


Fig. 13. For a plant to be a chimera, the mutation must occur in the shoot apical initials or close to them. Based on the spatial position of the mutation, there are three recognized types of chimeras: periclinal chimeras are formed by a mutation of a tunica initial cell that spreads through a whole tunica layer, forming a genetically distinct layers of cells in the SAM, mericlinal chimeras are formed in a subapical position in the tunica and spread in the tunica layer, but do not cover the entire SAM and (c) sectorial chimeras either have a heterogenomic population of cells traversing multiple SAM layers or have non-patterned heterogenomic patches of cells. (6)

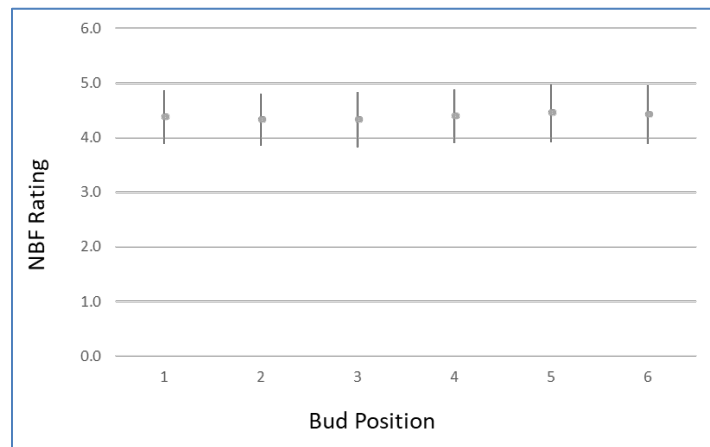


Fig. 14. NBF average ratings with standard deviations for severely affected trees (NBF score of 4-5) at the end of the seven-year field study.

References.

1. Kester, D.E., K.A. Shackel, W.C. Micke, M. Viveros, and T.M. Gradziel. (2004). Noninfectious bud failure in 'Carmel' almond: I. Pattern of development in vegetative progeny trees. *J. Amer. Soc. Hort. Sci.* 129(2):244-249.
2. Fernandez i Marti, A., Gradziel, T. M. and Socias i Company, R. 2014. Methylation of the Sf locus in almond is associated with S-RNase loss of function. *Plant Molecular Biology* 86: 681-689.
3. Akagi, T, Hanada,T, Yaegaki, H, Gradziel, T, and Ryutaro Tao, R. 2016. Genome-wide view of genetic diversity reveals paths of selection and cultivar differentiation in peach domestication. *DNA Research*,1–12.
4. Hanada, T; A. Watari, T. Kibe, H. Yamane, A. Wünsch, T.M. Gradziel, Y. Sasabe, H. Yaegaki, M. Yamaguchi and R. Tao. 2017. Two Novel Self-compatible S Haplotypes in Peach (*Prunus persica*). *J. Japan. Soc. Hort. Sci.* 83:203-213. DOI 2503/jjshs1.CH-099.
5. Su, M. N., Venkatachalam, M., Gradziel, T. M., Liu, C. Q., Zhang, Y., Roux, K. H. and Sathe, S. K. 2017. Application of mouse monoclonal antibody (mAb) 4C10-based enzyme-linked immunosorbent assay (ELISA) for amandin detection in almond (*Prunus dulcis* L.) genotypes and hybrids. *LWT - Food Science and Technology* 60: 535-543. 60 (2015) 535e543.
6. Nassar, N.M.A. , N. N. Bomfim Fernandes, , D. Y. Hashimoto Freitas. and T. M. Gradziel Interspecific Periclinal Chimeras as a Strategy for Cultivar Development. 2017. In J. Janick (ed.) *Plant Breeding Reviews*. 40:235-263. ISBN: 978-1-119-27968-6
7. Jonathan Fresnedo-Ramírez, Thomas R. Famula and Thomas M. Gradziel. 2017. Application of a Bayesian ordinal animal model for the estimation of breeding values for the resistance to *Monilinia fruticola* (G.Winter) Honey in progenies of peach [*Prunus persica* (L.) Batsch]. *Breeding Science Preview* doi:10.1270/jsbbs.16027
8. Fresnedo-Ramírez, J., Chan, H. M., Parfitt, D. E., Crisosto, C. H., & Gradziel, T. M. 2017. Genome-wide DNA-(de)methylation is associated with Noninfectious Bud-failure exhibition in Almond (*Prunus dulcis* [Mill.] D.A.Webb). *Scientific Reports*, 7. doi:10.1038/srep42686.
9. Gradziel T, B. Lampinen and J.E. Preece. (2019). Propagation from Basal Epicormic Meristems Remediate an Aging-Related Disorder in Almond Clones. *Horticulturae* 2019, 5(2), 28; <https://doi.org/10.3390/horticulturae5020028>
10. Gradziel, t. and J. Fresnedo-Ramírez. (2019). Noninfectious Bud-failure As a Model for Studying Age Related Genetic Disorders in Long-Lived Perennial Plants. *Journal of the American Pomological Society* 73(4): 240-253 2019.

11. D'Amico-Willman, K. M., Niederhuth, C. E., Willman, M. R., Gradziel, T. M., Ouma, W. Z., Meulia, T., et al. (2021). Integrated analysis of the methylome and transcriptome of twin almonds (*Prunus dulcis* [Mill.] D.A. Webb) reveals genomic features associated with non-infectious bud failure. doi: <https://www.doi.org/10.1101/2021.02.08.430330>. D'Amico-Willman, K.M. , Gina M. Sideli, Brian J. Allen, Elizabeth S. Anderson, Thomas M. Gradziel, Jonathan Fresnedo-Ramírez. Identification of putative markers of noninfectious bud failure in almond (*Prunus dulcis* [Mill.] D.A. Webb) through genome wide DNA methylation profiling and gene expression analysis in an almond × peach hybrid population. *Frontiers Front. Plant Sci.* 13:804145. doi: 10.3389/fpls.2022.804145.
12. D'Amico-Willman, K.M. Chad E. Niederhuth, Elizabeth S. Anderson, Thomas M. Gradziel, Jonathan Fresnedo Ramírez. 2021. Hypermethylation is associated with increased age in almond (*Prunus dulcis* [Mill.] D.A. Webb) accessions. *bioRxiv* 2021.05.02.442365; doi: <https://doi.org/10.1101/2021.05.02.442365>
13. D'Amico-Willman, K.M.; Anderson, E.S.; Gradziel, T.M.; Fresnedo-Ramírez, J. Relative Telomere Length and Telomerase Reverse Transcriptase (TERT) Expression Are Associated with Age in Almond (*Prunus dulcis* [Mill.] D.A. Webb). *Plants* 2021, 10, 189. <https://doi.org/10.3390/plants10020189>
14. Gradziel, T.M.; Shackel, K.A. 2021. Propagation of an Epigenetic Age-Related Disorder in Almond Is Governed by Vegetative Bud Ontogeny Rather Than Chimera-Type Cell Lineage. *Horticulturae*, 7, 190. <https://doi.org/10.3390/horticulturae7070190>

Progress report on a research grant proposal to: Fruit Tree, Nut Tree and Grapevine Improvement Advisory Board (IAB)

April 7, 2021

Project Title: Study of the Effects of Little cherry virus-1 and Little cherry virus-2 on Different Cherry Rootstocks

Fiscal Year: 2020-2021, fourth year

Project Leader: Maher Al Rwahnih, Academic Administrator, Department of Plant Pathology, Foundation Plant Services, University of California,

Objectives:

1. To test a collection of plants by RT-qPCR to locate infected source material needed for the experiment.
2. To evaluate the effects of LChV-1 and LChV-2 on 16 different popular *Prunus* rootstocks. All rootstocks will be grafted with the same cherry scion cultivar, 'Bing'.
3. To test the inoculated plants in year 2 for the selected viruses and monitor the virus movement and record the symptom observation.

Accomplishments:

Objective 1: To test a collection of plants by RT-qPCR to locate infected source material needed for the experiment.

In the first year of this project, two selections were chosen to serve as the inoculation source for LChV-1 and LChV-2. We identified a single infection source of LChV-1 but were unable to do so for LChV-2. The inoculation source that we selected is co-infected with CVA. Healthy 'Bing' cherry trees from our Foundation nursery were T-bud inoculated with virus positive material from the source trees. Four trees were inoculated for each virus treatment to supply us with LChV-1 and LChV-2 infected 'Bing' buds for our grafting experiments.

The work for this objective has been accomplished.

Objective 2: To evaluate the effects of LChV-1 and LChV-2 on 16 different popular Prunus rootstocks. All rootstocks will be grafted with the same cherry scion cultivar, 'Bing'.

Grafting of infected 'Bing' scion material into container grown rootstocks in May and October of 2018 had a high incidence of failed bud take owing likely to the slender rootstock material in containers not accepting the relatively large bud material from trees growing in the field.

In May 2020 (third year of funding), 501 trees, described in Figure 1, that tested negative for LChV-1 or LChV-2 movement into the rootstock (light blue and light pink boxes) were regrafted with virus-infected material. Trees were observed in October 2020 (fourth year of funding) for successful growth of new grafts. Budtake was successful in 42% of grafts; 58% failed and will need to be regrafted.

January 2021

The field crew pruned the rootstock back to about 5 nodes to prepare for the regrafting. The virus source trees were pruned and all graftable material collected 500 buds of Bing were collected from the Foundation trees

In April 2021 (fourth year of funding), any trees that do not exhibit 'Bing' scion growth, will be regrafted.

Objective 3: To test the inoculated plants in year 2 for the selected viruses and monitor the virus movement and record the symptom observation.

Following bud break in 2019, bud graft status, for 1st and 2nd graft iterations, was recorded as either dead, alive or growing. Additionally, in September of 2019 (third funded year), leaf petioles from rootstock branches growing above the graft site were tested by RT-qPCR for graft transmission of LChV-1 or LChV-2. The results of RT-qPCR are shown in Figure 1.

Plant Representation- Olmo Area Block B

Block B Row 1	1	2	-	4	5	6	7	8	9	-	11	12	13	14	15	-	17	18	-	20	21	22	23	24	25	26	27	28	29	30
Block B Row 2	1	2	3	4	5	6	7	8	9	10	11	12	13	14	15	-	-	-	-	-	21	22	23	24	25	26	27	28	29	30
Block B Row 3	1	2	3	4	5	6	7	8	9	10	11	12	13	14	15	16	17	18	19	20	21	22	23	24	25	-	27	28	29	30
Block B Row 4	1	2	3	4	5	6	7	8	9	10	11	12	13	14	15	16	17	18	19	20	21	22	23	24	25	26	27	28	29	30
Block B Row 5	1	2	3	4	5	6	7	-	9	-	11	12	-	14	15	16	17	18	19	20	21	22	-	24	25	26	27	-	29	
Block B Row 6	1	2	3	4	-	-	-	-	-	-	11	12	13	14	15	16	17	18	19	20	21	22	23	24	25	26	27	28	29	30
Block B Row 7	1	2	3	4	5	6	7	8	9	10	11	12	13	14	15	16	17	18	19	20	21	22	23	24	25	26	27	28	29	30
Block B Row 8	1	2	3	4	-	6	7	8	9	10	11	12	13	14	15	16	17	18	19	20	21	22	23	24	25	26	-	-	29	30
Block B Row 9	1	2	3	4	5	6	7	8	9	10	11	12	13	14	15	16	17	18	19	20	21	22	23	24	25	26	27	28	29	30
Block B Row 10	1	2	3	4	5	6	7	8	9	10	11	12	13	14	-	16	17	18	19	20	21	22	23	24	25	26	27	28	29	30
Block B Row 11	1	2	3	4	5	6	7	8	9	10	11	12	13	14	15	16	17	-	19	20	21	22	23	24	25	26	27	28	29	30
Block B Row 12	1	2	3	4	5	6	7	8	9	10	11	12	13	14	15	16	17	18	19	20	21	22	23	24	25	26	27	28	29	30
Block B Row 13	1	2	3	4	5	6	7	-	9	-	11	12	13	14	15	16	17	18	19	20	21	22	23	24	-	26	27	28	29	30
Block B Row 14	1	2	3	4	5	6	7	8	9	10	11	12	13	14	15	16	17	18	19	20	21	22	23	24	25	26	27	28	29	30
Block B Row 15	1	2	3	4	5	6	7	8	9	10	-	-	-	-	-	16	17	18	19	20	21	22	23	24	25	26	27	28	29	30
Block B Row 16	1	2	3	4	5	6	7	8	9	10	11	12	13	14	15	16	17	18	19	20	21	22	23	24	25	26	27	28	29	30
Block B Row 17	1	2	3	4	-	6	7	8	9	10	11	12	13	14	15	16	17	18	19	20	21	22	23	24	25	26	27	28	29	30
Block B Row 18	1	2	3	4	5	6	7	8	9	10	11	12	13	14	15	-	17	18	19	20	21	22	23	24	25	-	-	-	29	30
Block B Row 19	1	2	3	4	5	6	7	8	9	10	11	12	13	14	15	16	17	18	19	20	21	22	23	24	25	26	27	28	29	30
Block B Row 20	1	2	3	4	5	6	7	8	9	10	11	12	13	14	15	16	17	18	19	20	21	22	23	24	-	26	27	28	29	30
Block B Row 21	1	2	-	4	5	6	7	8	9	10	11	12	13	14	15	16	17	18	19	20	21	22	23	24	25	26	27	28	29	30
Block B Row 22	1	2	3	4	5	6	-	8	9	10	11	12	13	14	15	16	17	-	-	-	21	22	23	24	25	26	27	28	29	30
Block B Row 23	1	2	3	4	5	6	7	8	9	10	11	12	13	14	15	16	17	18	19	20	21	22	23	24	25	26	27	28	29	30
Block B Row 24	-	-	-	4	-	6	7	8	9	10	11	12	13	14	15	16	17	18	19	20	21	22	23	24	25	26	27	28	29	30
Block B Row 25	1	-	-	-	5	6	7	8	9	10	11	12	13	14	15	16	17	18	19	20	21	22	23	24	25	26	27	28	29	30
Block B Row 26	1	2	3	4	5	6	7	8	9	10	11	12	13	14	15	16	17	18	19	20	21	22	23	24	25	26	27	-	29	
Block B Row 27	1	2	3	4	5	6	7	8	9	10	11	12	13	14	15	16	17	18	19	20	21	22	23	24	25					
Block B Row 28	1	2	3	4	5	6	7	8	9	10	11	12	-	-	15	16	17	18	19	20	21	22	23	24	25	26	27	28	29	30
Block B Row 29	1	-	3	4	5	6	7	8	9	10	11	12	13	14	15	16	17	18	19	20	21	22	23	24	25	26	-	28	29	30
Block B Row 30	1	2	3	4	5	6	7	8	9	10	11	12	13	14	15	-	17	-	-	-	21	22	23	24	25	26	27	28	29	30
Block B Row 31	1	2	3	4	5	-	-	-	-	-	-	-	-	-	-	-	17	18	19	20	21	22	23	24	-	26	27	-	29	30
Block B Row 32	1	2	3	4	5	6	7	8	9	10	11	12	13	14	15	16	17	18	19	-	21	22	23	24	25	26	27	28	29	
Block B Row 33	-	-	3	-	-	7	-	-	-	-	11	12	13	14	15	16	-	18	19	20	21	22	23	24	25	26	27	28	29	
Block B Row 34	1	2	3	4	5	6	7	8	9	10	11	12	13	14	15	16	17	18	19	20	21	22	23	24	25	26	27	28	29	30
Block B Row 35	1	2	3	4	5	6	7	8	9	10	11	12	13	14	15	-	17	18	-	-	21	22	23	24	25	26	27	28	29	30
Block B Row 36	1	2	3	4	5	6	7	8	9	10	11	12	13	14	15	16	17	18	19	20	21	22	23	24	25	26	27	28	29	30
Block B Row 37	1	2	3	4	5	6	7	8	9	10	11	12	-	14	15	16	17	18	19	20	21	22	23	24	25	26	27	28	29	30
Block B Row 38	1	2	3	4	5	6	7	8	9	10	11	12	13	14	15	16	17	-	19	20	21	22	23	24	25	26	27	28	29	
Block B Row 39	1	2	3	4	5	6	7	8	9	10	11	12	13	14	15	16	17	18	19	20	21	22	23	24	25	26	27	-	29	30
Block B Row 40	1	2	3	4	5	6	7	8	9	10	11	-	-	14	-	16	17	18	19	20	21	22	23	24	25	26	27	28	29	30
Block B Row 41	1	2	3	4	5	6	7	8	9	-	-	-	-	-	-	-	17	18	19	20	21	22	23	24	25	26	27	28	29	30
Block B Row 42	1	2	3	4	5	6	7	8	9	10	11	12	13	14	15	16	17	18	19	-	21	-	23	24	-	26	27	28	29	30

Figure 1. The randomized block of rootstocks grafted with healthy, LChV-1 or LChV-2 infected Bing scion in the spring and fall iterations. The grey boxes represent plants grafted with healthy Bing scion or ungrafted controls. The dark blue boxes represent plants with successful grafting and transmission of LChV-1. The light blue boxes represent plants with unsuccessful grafting and/or negative RT-qPCR results for LChV-1. The dark salmon boxes represent plants with successful grafting and transmission of LChV-2. The light pink boxes represent plants with unsuccessful grafting and/or negative RT-qPCR results for LChV-2. White areas represent plants that died.

In September of 2021 (extension of fourth year of funding), leaf petioles from leaves growing on the root stock above the graft site of all trees that tested LChV-1 or LChV-2 negative in 2019 will be sampled and tested by RT-qPCR to see if recent grafting (in May 2020 or April 2021) was successful in introducing the virus into the rootstock. This data allows us to correlate the presence of the virus with any symptoms recorded.

A three month no cost extension of our fourth-year grant was requested to allow us to complete this objective.

All trees will be observed for two years following successful grafting for signs of hypersensitive response of the rootstock to LChV-1 or LChV-2. We will evaluate for visual symptoms of tree death, gumming, leaf distortion, leaf color and vigor. Based on these observations, the reaction of the rootstocks to the virus will be categorized as lethal (died in the presence of the virus), severe (strong adverse response, but non-lethal within two years), sensitive (mild virus symptoms noted but the tree not affected severely), and tolerant (no symptoms). If deemed necessary some plants with suspicious symptoms will be sacrificed, the trunk will be autoclaved to remove the bark and examine the wood for wood marking symptoms.

The field will continue to be maintained and pesticides will be applied frequently to ensure mealybugs do not invade the field, as they can spread LChV-2.

Summary:

Little cherry disease (LCD), associated with Little cherry virus-1 (LChV-1) or -2 (LChV-2), is a common problem of cherries (*Prunus avium*) which occurs worldwide, causes unmarketable fruit and often results in tree or orchard removal (Jelkmann and Eastwell, 2011). Most of the new cherry rootstocks used in cherry production are interspecific *Prunus* hybrids which introduces an increased risk of an adverse reaction (hypersensitivity) to some viruses (Lang and Howell, 2001). Hypersensitive reactions exhibit graft union gum exudation, premature abscission, and tree death within one or two growing seasons and have been shown to occur in *Prunus* when infected with Prunus necrotic ringspot virus (PNRSV) and Prune dwarf virus (PDV) (Howell and Lang, 2001, Lang and Howell, 2001, Lang et al., 1998). We propose to evaluate the effects of LChV-1 and LChV-2 on 16 different popular *Prunus* rootstocks. All rootstocks will be grafted with a scion variety from the same accession. Observations of budtake and tree performance will be recorded and evaluated for two years. Rootstocks will be rated for sensitivity to LChV-1 and LChV-2 and this information will be shared with growers and nurseries to assist in making rootstock selection decisions.

Project's Benefit to Nursery Industry:

In the US, sweet cherry fresh market production totaled 254,906 tons and was valued at \$703 million in 2015 (NASS, 2017). Washington, California and Oregon account for more than 90% of sweet cherry industry in the US, with 34,786, 34,742, and 13,416 acres planted to sweet cherries in 2012, respectively (NASS, 2017). Interest in sweet cherry production has increased in recent years due to the high value of fresh market cherries and the increasing availability premium quality varieties and new rootstocks with exciting horticultural traits (Lang and Howell, 2001).

Little cherry disease is a concern to growers wherever cherries are grown. LCD is associated with LChV-1 or LChV-2, which can be found in single and mixed infections. Trees with LCD produce cherries of small size and poor color making fruit unmarketable. The problem results in unpicked limbs or trees, tree removal and even orchard removal. The disease is readily transmitted by grafting and LChV-2 is vectored by mealybugs (Jelkmann and Eastwell, 2011). To date, no breeding programs have been successful in finding resistance to the disease.

In orchards worldwide, cherries (*P. avium*) are either budded or grafted onto rootstocks. Rootstocks provide protection from soil-borne pests and improved tolerance to abiotic stresses, such as heavy soils, drought conditions, salinity, and cold winter temperatures, thus, increasing the survival of the scion material. Traditionally, cherries in the US were grown on Mazzard or Mahaleb rootstocks or clonally-propagated 'Colt' which are generally tolerant of infection by pollen-borne viruses, PDV and PNRSV (Lang et al. 1998). It has been increasingly well-documented that new *Prunus* rootstock selections can show hypersensitive reactions to viruses that have been typically well tolerated by traditional rootstocks (Lang et al. 1997, Lang et al. 1998, Lang and Howell 2001, Howell and Lang 2001). These new rootstock selections are derived from species other than or are hybrids with *P. avium* which offers genetic diversity and novel horticultural traits, but with an increased risk of hypersensitivity. Hypersensitive (rapid and lethal) reactions exhibit graft union gum exudation, premature abscission, and tree death within one or two growing seasons. Viruses with documented hypersensitivity include PNRSV and PDV (Howell and Lang, 2001). It is not currently known if LChV-1 and LChV-2 can cause similar hypersensitive reactions in the common *Prunus* rootstocks.

We plan to conduct a field trial to investigate hypersensitivity reactions to LChV-1 and LChV-2 in the top *Prunus* rootstocks. Currently, we anticipate using GiSelA®3, GiSelA®5, GiSelA®6, GiSelA®12, Krymsk®5, Krymsk®6, Krymsk®7, EMLA Colt, MaxMa®14, Cass, Clare, Clinton, Crawford, Lake and seedlings of Mazzard and Mahaleb in the trial. We will assess the sensitivity of these rootstocks to LChV-1 and LChV-2 and share the results of our research.

This research has a great benefit to the cherry growing industry as the results of our research will assist growers and nurseries in rootstock selection for new plantings. Informed rootstock selection will result in healthier, more productive cherry trees.

**Final report on a research grant proposal to: Fruit Tree, Nut Tree and Grapevine
Improvement Advisory Board (IAB)**

March 31, 2022

Project Title: Development and validation of real-time quantitative PCR assays for the detection of fruit tree viruses

Project Duration: 07/01/2020 to 06/30/2021

Project Leader: Maher Al Rwahnih, Academic Administrator, Department of Plant Pathology, Foundation Plant Services, University of California,

Objectives:

1. Evaluate currently available real-time qPCR assays and screen select fruit tree populations for targeted pathogens to compile a representative set of isolates.
2. Incorporate new genetic data into a more complete characterization of genetic variation across the targeted pathogens to inform assay design.
3. Construct improved assays utilizing multiple primers/probes sets for detecting all existing targeted pathogen variants.
4. Empirically test and validate proposed assay designs using positive controls.
5. Disseminate research progress and results.

Accomplishments:

Objective 1:

Previously published real-time quantitative PCR (qPCR)-based assays for targeted pathogens (Table 1) were evaluated *in silico* to determine their detection capacity, i.e., number of isolates that they can detect, using the available sequence data in GenBank and bioinformatics programs. In the case of ACLSV, ApMV, ASGV, ASSVd, CGRMV, CRLV, LChV-1, LChV-2, PDV, PNRSV and ToRSV assays (Table 2), sequence comparisons showed nucleotide mismatches between primers/probes of the existing corresponding assays and the alignment generated for each virus. Nucleotide mismatches observed during these analyses ranged from 1 to 10, suggesting that additional primers and probes needed to be added to existing assays or that assays needed to be redesigned in a more conserved region of the genome to avoid potential detection failures. In contrast, the pear decline phytoplasma and CLRV assays (Hodgetts et al. 2009; Osman et al. 2014) did not display nucleotide mismatches, indicating that modifications were not needed. In the case of ASPV, ArMV, and TRSV no qPCR-based assays exist.

Table 1. Targeted pathogens of fruit trees included in the initial research proposal.

Disease	Disease Agent	Host
Apple chlorotic leaf spot	Apple chlorotic leafspot virus (ACLSV)	Pome, <i>Prunus</i>
Apple mosaic	Apple mosaic virus (ApMV)	Pome, <i>Prunus</i>
Apple stem grooving	Apple stem grooving virus (ASGV)	Pome
Apple stem pitting, Pear stem pitting, Pear stony pit disease	Apple stem pitting virus (ASPV)	Pome
Flat apple disease	Cherry rasp leaf virus (CRLV)	Pome, <i>Prunus</i>
Tobacco ringspot	Tobacco ringspot virus (TRSV)	Pome
Apple union necrosis	Tomato ringspot virus (ToRSV)	Pome, <i>Prunus</i>
Pear decline	Pear decline Phytoplasma	Pome
Apple scar skin/Dapple apple disease	Apple scar skin viroid (ASSVd)	Pome
Pear blister canker	Pear blister canker viroid (PBCVd)	Pome
Cherry green ring mottle	Cherry green ring mottle virus (CGRMV)	<i>Prunus</i>
Cherry leafroll	Cherry leafroll virus (CLRV)	<i>Prunus</i>
Little cherry	Little cherry virus 1 (LChV-1)	<i>Prunus</i>
Little cherry	Little cherry virus 2 (LChV-2)	<i>Prunus</i>
Prune dwarf	Prune dwarf virus (PDV)	<i>Prunus</i>
Prunus necrotic ringspot	Prunus necrotic ringspot virus (PNRSV)	<i>Prunus</i>
Arabis mosaic	Arabis mosaic virus (ArMV)	<i>Prunus</i>

Table 2. Published real-time qPCR-based assays for targeted pathogens of fruit trees.

Pathogen	Citation of Published Assay
ACLSV	Osman et al. 2016
ApMV	Osman et al. 2014
ASGV	Gadiou and Kundu 2012
ASSVd	Kim et al. 2010
CGRMV	Osman et al. 2016
CRLV	Osman et al. 2016
LChV-1	Katsiani et al. 2018
LChV-2	Jelkmann et al. 2006
PDV	Osman et al. 2014
PNRSV	Osman et al. 2014
ToRSV	Osman et al. 2014

In addition to the 17 different pathogens included in the initial research proposal, 11 additional pathogens (Table 3) and their corresponding detection assays were investigated *in silico* during the second year of this project. The CNRMV, CVA, and PBNPaV assays and their corresponding assays contained nucleotide mismatches that could result in detection failures (Figure 1), requiring an update to these assays. No published real-time qPCR-based assays existed for the remaining eight pathogens (Table 3).

Table 3. Pathogens added during the second year of the project and the three currently available real-time qPCR-based assays. NA means no available assay.

Pathogen	Acronym	Assay Citation
Apple green crinkle associated virus	AGCaV	NA
Apple hammerhead viroid	AHVd	NA
Apple rubbery wood virus 1 & 2	ARWV 1 & 2	NA
Cherry necrotic rusty mottle virus	CNRMV	Osman et al. 2016
Cherry rusty mottle associated virus	CRMaV	NA
Cherry virus A	CVA	Osman et al. 2016
Citrus concave gum-associated virus	CCGaV	NA
Nectarine stem pitting-associated virus	NSPaV	NA
Nectarine virus M	NVM	NA
Peach mosaic virus	PcMV	NA
Plum bark necrosis stem pitting-associated virus	PBNPaV	Lin et al. 2013

Figure 1. Potential detection failures caused by nucleotide mismatches in the CNRMV assay and different CNRMV isolates. Isolates with more than two mismatches are shown in grey.

Number of CNRMV Isolate Sequences	Number of Mismatches in CNRMV Assay	Assay Sequence
65	0	CTCAACATTGCATCTGAT
1	1	CTCAACATTGCA A CTGAT
8	1	CTCAACATTGCAG C TGAT
56	3	CTCAAT T AT C GC C TCTGAT
2	3	CTCAAT T AT C GC T TCTGAT
19	3	CT T AACATTGC C TCTG A A
28	4	CT T AAT T AT C GC C TCTGAT
1	5	CT T AAT T AT C GC CC TGAT

Plant material allegedly infected by all the targeted pathogens (Tables 1 and 3) was obtained from the Foundation Plant Services (FPS) and the Clean Plant Center Northwest (CPCNW) introduction pipelines. Both collections include foreign and domestic selections of *Prunus* and pome fruit trees. In total, 214 samples (Table 4) were obtained and included in the pathogen screening via high throughput sequencing (HTS). As a result, multiple isolates were identified for all the pathogens (Table 5), except for NVM, PcMV, CRMaV, ToRSV, TRSV and ARWV 1 & 2. Only one isolate was identified for each of these viruses.

Table 4. Fruit tree samples analyzed by high throughput sequencing (HTS).

Fruit Tree	Number of Samples
Almond	3
Apple Rootstock	17
Apricot	2
Cherry	35
Cherry Rootstock	5
Miscellaneous Prunus Species	12
Nectarine	8
Peach	34
Pear	21
Pear Rootstock	5
Plum/prune	22
Apple	50

Table 5. Number of isolates obtained for each targeted fruit tree pathogen.

Acronym	Number of Isolates
ACLSV	24
AGCaV	18
AHVd	8
ApMV	5
ASGV	24
ASPV	39
ASSVd	2
ARWV 1 & 2	1
ArMV	2
CGRMV	9
CLRV	2
CNRMV	4
CRLV	2
CRMaV	1
CVA	24
CCGaV	3
LChV-1	3
LChV-2	3
NSPaV	2
NVM	1
PcMV	1
Pear decline phytoplasma	2
PBCVd	8
PBNSPaV	10

PDV	16
PNRSV	19
ToRSV	1
TRSV	1

Objective 2:

All the new HTS data generated was analyzed using the FPS in-house bioinformatics pipeline, a local UNIX server-based high throughput viral meta-genomics pipeline. This analysis provided several complete and near-complete genomes of the following viruses and viroids: ACLSV, ApMV, ASSVd, ASGV, ASPV, PBCVd, PNRSV, LChV-1, LChV-2, PBNSPaV, and CGRMV. This sequence data has been submitted to GenBank, providing a more complete characterization of the genetic variation for these pathogens.

Objective 3:

Twenty-four new or updated real-time qPCR-based assays were developed during this study (Table 6). Additional primers or probes were added to the previously published assays when more than two nucleotide mismatches were detected during *in silico* analyses. These updates included assays for ACLSV, CRLV, LChV-1, PDV, ToRSV and ApMV. Adjustments to these assays primarily involved adding one extra probe and/or up to two extra primers.

Table 6. Updated or newly designed assays for detection of pathogens infecting fruit trees.

Pathogen	Type of Primer	Number of Primers	Target Region	Reference	Note
ToRSV	Forward	2	CP/Polyprotein	Osman et al. 2014	Updated
	Reverse	2			
	Probe	1			
ArMV	Forward	2	CP/Polyprotein	This study	
	Reverse	1			
	Probe	2			
ApMV	Forward	4	CP	Osman et al. 2014	Updated
	Reverse	2			
	Probe	2			
ACLSV	Forward	1	CP	Osman et al. 2017	Updated
	Reverse	5			
	Probe	2			
LChV1	Forward	4	CP	Katsiani et al. 2018	Updated
	Reverse	1			
	Probe	2			
LChV2	Forward	2	RdRp	This study	
	Reverse	1			
	Probe	2			

CRLV	Forward	1	RdRp	Osman et al. 2017	Updated
	Reverse	2			
	Probe	2			
PDV	Forward	4	CP	Osman et al. 2014	Updated
	Reverse	2			
	Probe	2			
PNRSV	Forward	4	CP	This study	
	Reverse	2			
	Probe	2			
CGRMV	Forward	2	TGB1	This study	
	Reverse	1			
	Probe	1			
PBCVd	Forward	3	Viroid genome	This study	
	Reverse	4			
	Probe	2			
ASSVd	Forward	5	Viroid genome	This study	
	Reverse	4			
	Probe	2			
ASPV	Forward	5	CP	This study	
	Reverse	5			
	Probe	2			
TRSV	Forward	3	CP	This study	
	Reverse	3			
	Probe	2			
ASGV	Forward	2	MP/Polyprotein	This study	
	Reverse	1			
	Probe	1			
PBNSPaV	Forward	1	3' UTR	This study	
	Reverse	1			
	Probe	1			
CVA	Forward	3	CP	This study	
	Reverse	2			
	Probe	2			
AHVd	Forward	3	Viroid genome	This study	
	Reverse	3			
	Probe	1			
NVM	Forward	1	RdRp/Polyprotein	This study	
	Reverse	2			
	Probe	1			

NSPaV	Forward	2	CP	This study	
	Reverse	2			
	Probe	1			
CNRMV	Forward	1	CP	This study	
	Reverse	1			
	Probe	1			
ARWV 1	Forward	1	RdRp	This study	
	Reverse	1			
	Probe	1			
ARWV 2	Forward	1	RdRp	This study	
	Reverse	1			
	Probe	1			
CRMaV	Forward	2	CP	This study	
	Reverse	2			
	Probe	1			
AGCaV	Forward	2	CP	This study	
	Reverse	2			
	Probe	1			
CCGaV	Forward	1	RdRp	This study	
	Reverse	1			
	Probe	1			
PcMV	Forward	1	RdRp	This study	
	Reverse	2			
	Probe	1			

Our HTS nucleotide sequence data indicated that the genomic regions targeted by the published assays for LChV-2, CNRMV, CVA, PNRSV, ASGV, ASSVd, CGRMV and PBNSPaV were not as conserved as previously thought. *In silico* analyses indicated that other regions were more conserved so new assays were designed accordingly (Table 6).

Finally, no real time qPCR-based assays existed for NSPaV, NVM, AHVd, ASPV, ArMV, PBCVd, TRSV, CRMaV, PcMV and ARWV 1 & 2. We designed assays specific to these pathogens using a custom scrip and a multi-step process (Fig. 2). This script identified potential candidates for primers/probes, which were then adjusted according to the parameters specific for TaqMan™ real-time qPCR-based assays.

Figure 2. The design process for the new real-time qPCR-based assays using TRSV as an example.

Virus/Viroid Oligo	Automatic analysis by custom script		Manual analysis using Primer Express	Manual analysis using MUSCLE	Primer Name	To Order Primers/Probes	Target Region
	Original Primer/Probes (Frequency)	Adjusted Primers/Probes	Final Sequences (*Reverse)				
TRSV	Forward	AGGTCTAAACAGGCCCAAGGCTCA 14 AGGTCTAAACAGGCCCAAGGCCCA 4 AGTTCACAAACAGGCCCAAGGCTCA 8 AGGACTAAACAGGCCCAAGGCTCA 3	TCTAAACAGGCCCAAGGCTCA CTAAACAGGCCCAAGGCC CAACAGGCCCAAGGCTCA ACTAAACAGGCCCAAGGCTCA	TCTAAACAGGCCCAAGGCTCA CTAAACAGGCCCAAGGCC CAACAGGCCCAAGGCTCA	TRSV-F1 TRSV-F2 TRSV-F3	TCTAAACAGGCCCAAGGCTCA CTAAACAGGCCCAAGGCC CAACAGGCCCAAGGCTCA	CP
	Probe	GATTGGGGTGCTTACTGGCAAGG 18 GATTGGGGTGCTTATTGGCAAGG 2 GATTGGGGTGCTTACTGGCAAGG 5 GACTGGGGTGCTTACTGGCAAGG 3 GATTGGGGGACTTACTGGCAAGG 1	GGTGCTTACTGGCAAGG GGTGCTTATTGGCAAGG GTGCCTACTGGCAAGG GGTGCTTACTGGCAAGG GAGCCTACTGGCAAGG	GTGCCTACTGGCAAGG	TRSV-P1	GTGCCTACTGGCAAGG	
	Reverse	GCTGGTGCAACGCCATCTGGTGC 5 GCTGGTGCGACGCCCAACTGGTGC 3 GCTGGTGCTACGCTTCTGGCGC 1 GCTGGTGCGACGCCATCTGGTGC 20	CTGGTGCAACGCCATCTG TGGTGCGACGCCCAACTG CTGGTGCTACGCTTCTGG TGGTGCGACGCCATCTG	CAGATGGCGTTGCACCAG CCAGAAGGCGTAGACCAG CAGATGGCGTCGCCCA	TRSV-R1 TRSV-R2 TRSV-R3	CAGATGGCGTTGCACCAG CCAGAAGGCGTAGACCAG CAGATGGCGTCGCCCA	

Objective 4:

The updated or new assays for pathogens included in Table 6 were initially evaluated using known positive and negative controls, demonstrating that these assays had high analytical sensitivity and specificity. The amplification efficiencies of the assays varied and ranged from 82% to 117%. Next, the assays were used to test plants that had been analyzed by HTS and shown to be infected by specific viruses in Table 6. The HTS and PCR test results were identical, verifying that the assays also had high diagnostic sensitivity and specificity.

For large scale validation of the assays, we collected tree samples from the USDA National Clonal Germplasm Repository near Winters, California. This is a *Prunus* germplasm collection of worldwide origin and contains approximately 4,000 *Prunus* trees representing different accessions. Trees in this collection include almonds, apricots, cherries, peaches, plums, and nectarines. We collected and tested 333 samples; 182 or 54.6% were positive for at least one of the viruses listed in Table 7. CLRV, CRLV, and CRMaV were not detected.

Table 7. Viruses identified in the National Clonal Germplasm Repository.

Virus	Number of Infected Trees	Percent Infected of Total (%)
ACLSV	19	5.7
CGRMV	20	6
CLRV	0	0
CNRMV	4	1.2
CRLV	0	0
CRMaV	0	0
CVA	39	11.7
LChV-1	10	3
LChV-2	3	0.9
NSPaV	4	1.2
NVM	10	3

PcMV	2	0.6
PBNSPaV	33	9.9
PDV	29	8.7
PNRSV	127	38.1

In the spring of 2020 and 2021, we tested 246 pear and apple samples from El Dorado and San Joaquin counties that were collected and sent to FPS by farm advisors with UCCE Extension. The samples represented 15 orchards and included the following apple varieties: Fuji, Honeycrisp, Gala, Golden Delicious, Winesap, Mutsu, Gold Rush, and Sierra Beauty. Barlett Pear was the only pear variety and there was also an unknown Asian pear variety. The number of samples that were positive using the new qPCR-based assays are listed in Table 8.

Table 8. Viruses identified in a survey of pome trees in El Dorado and San Joaquin counties.

Assay/Pathogen	Number of Infected Trees	Percent Infected of Total (%)
ACLSV	122	50.0
AGCaV	14	5.7
AHVd	65	26.4
ApMV	0	0.0
ARWV1	1	0.4
ARWV2	98	40.0
ASGV	126	51.2
ASPV	125	50.8
ASSVd	0	0.0
CCGaV	35	14.2
CRLV	0	0.0
PBCVd	14	5.7
ToRSV	3	1.2
TRSV	0	0.0

ASGV, ASPV, ACLSV, ARWV2, and AHVd were the most common pathogens detected followed by CCGaV, PBCVd, AGCaV, ToRSV, and ARWV1. No positive samples were detected for ApMV, ASSVd, CRLV, and TRSV.

Objective 5:

Preliminary results have been presented during growers meetings organized by the UC Cooperative Extension, and scientific meetings organized by the California Department of Food and Agriculture (CDFA). This work is especially timely as the development of these more robust fruit trees pathogen detection assays concurs with recent changes to the CDFA Pome Registration and Certification Program in anticipation of creating a program at FPS that harmonizes with other state's pome industries. FPS is working closely with the CPCNW to standardize the testing process of new domestic and foreign fruit tree introductions.

In addition, the novel detection tools will be shared with diagnostic labs involved in the fruit tree industry in the US, including the National Clean Plant Network. Any assay we develop out of this project will be made available to CDFA and private commercial diagnostic labs and will augment the production of certified propagation material and the effective control of fruit tree pathogens in California and beyond. Finally, a scientific article describing several of these improved assays was recently published in *Plants* 2020, 9(2), pp. 273-286 titled, “Comprehensive real-time RT-PCR assays for the detection of fifteen viruses infecting *Prunus* spp.”.

Summary:

The CDFA is currently working to update the Pome Fruit Tree Registration and Certification regulations to create regulations that are harmonized with other state’s pome industries. In coordination with this effort, we investigated the qPCR-based assays that were available to detect viruses, viroids, and phytoplasmas targeted by the pome fruit working group, as well as the important *Prunus* pathogens. Our objectives were to screen select pome and *Prunus* tree populations for targeted pathogens to compile a representative set of isolates, evaluate current published assays, incorporate new genetic data into a more complete characterization of genetic variation across the targeted pathogens to inform assay design, construct improved assays utilizing multiple primers/probes sets for detecting all existing targeted pathogen variants, empirically test and validate proposed assay designs using positive controls, and disseminate research progress and results. The final product of this work is a large set of robust qPCR-based assays that detect the major pathogens of pome and *Prunus* fruit trees and therefore, ensure that high quality nursery planting stock is free from these pathogens.

**Final report on a research grant proposal to: Fruit Tree, Nut Tree and Grapevine
Improvement Advisory Board (IAB)**

April 1, 2022

Project Title: Improved detection and evaluation of the biological significance of grapevine vitiviruses

Project Duration: 07/01/2020 to 06/30/2021

Project Leader: Maher Al Rwahnih, Academic Administrator, Department of Plant Pathology, Foundation Plant Services, University of California,

Objectives:

1. Construct new or improved individual RT-qPCR assays for all known grapevine vitiviruses.
2. Screen select grapevine populations for vitiviruses and validate improved RT-qPCR assays.
3. Construct a universal assay for all grapevine vitiviruses.
4. Empirically test and validate the universal assay using positive and negative controls.
5. Evaluate the biological effects of GVG, H, I, J, L and M on the common grapevine indicators.
6. Disseminate research progress and results.

Accomplishments:

Objective 1:

New RT-qPCR assays for GVG, GVH, GVI, GVJ, GVL, and GVM have been designed (Table 1). Validation of analytical sensitivity and specificity of these assays using positive and negative controls including grapevines infected with vitiviruses GVA to GVM as well as virus-free vines was carried out successfully. In the case of the recently discovered GVM, infected material was obtained from Dr. Olufemi J. Alabi (Texas A&M University) using Dr. Al Rwahnih's USDA-APHIS permit. Analysis of existing RT-qPCR assays for GVA, GVB, GVD, GVE, and GVF showed cross reaction of GVA and GVF assays. Therefore, available GenBank sequences of GVA and GVF were retrieved for redesigning the corresponding assays. Development of new primers and probes for these two viruses (Table 1) has been completed and the assays were validated using vitivirus-infected grapevines as described above. The validation demonstrated that the new GVA and GVF assays specifically and efficiently detected the respective viruses.

Table 1. Updated or newly designed qPCR-based assays for the detection of specific vitiviruses.

Pathogen	Primer Type	Number of Primers	Target Region	Reference
GVA	Forward	1	Coat protein	Osman et. al., 2013; Updated this study
	Reverse	1		
	Probe	1		
GVF	Forward	2	Movement protein	Al Rwahnih et. al., 2014; Updated this study
	Reverse	2		
	Probe	1		
GVG	Forward	2	Coat protein	Developed in this study
	Reverse	4		
	Probe	1		
GVH	GVH-F1	2	RNA-dependent-RNA-replicase	Developed in this study
	GVH-F2	2		
	GVH-R1	2		
GVI	GVI-F1	3	Coat protein	Developed in this study
	GVI-F2	3		
	GVI-F3	1		
GVJ	GVJ-F	1	RNA-dependent-RNA-replicase	Developed in this study
	GVJ-R	1		
	GVJ-P	1		
GVL	GVL-F1	1	Coat protein	Developed in this study
	GVL-R1	1		
	GVL-P1	1		
GVM	GVM-F1	1	Coat protein	Developed in this study
	GVM-R1	1		
	GVM-P1	1		

Objective 2:

We used the new developed RT-qPCR assays from Objective 1 to screen 1,946 grapevines from populations with a historical incidence of vitiviruses. These vines originated from the USDA National Clonal Germplasm Repository (NCGR) in Davis, CA; FPS domestic and quarantine material; and the University of California-Davis Virus Collection (DVC). The number of positive vines for each virus is listed in Table 2. GVJ and GVM were not detected in any of the vines.

Table 2. Number of vines that were identified as being positive for a vitivirus using the newly developed RT-qPCR assays.

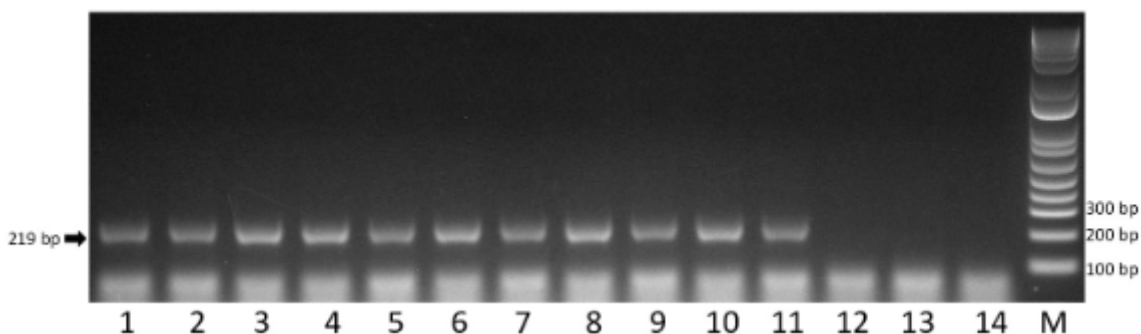
Vitivirus	Number of positive vines
GVG	8
GVH	60
GVI	16
GVJ	0
GVL	20

GVM	0
-----	---

Objective 3:

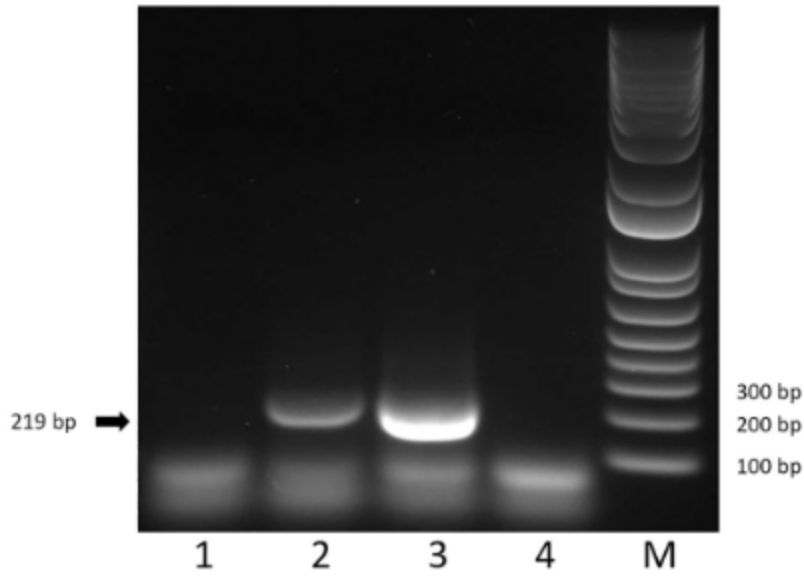
To certify grape material for propagation as virus tested, a universal RT-PCR assay that detects all known vitiviruses is desirable. To design this assay, multiple grapevine vitivirus sequences were aligned at the amino acid level to search for conserved motifs. Two highly conserved motifs were found at an ideal distance for RT-PCR detection in the RNA-dependent RNA polymerase region of the replicase protein. The amino acid motifs were back translated to create degenerate primers and used to successfully amplify all 11 grapevine vitiviruses (Fig. 1). The RT-PCR primers were also tested for their exclusivity by testing vines infected with closely related viruses in the *Betaflexiviridae* family, i.e., grapevine Pinot gris virus and grapevine rupestris stem pitting-associated virus, for exclusivity. No product was amplified for these two viruses (Fig. 1).

Figure 1. Detection of different grapevine vitiviruses by RT-PCR using the universal assay. Lane 1, grapevine virus 2; lane 2, grapevine virus B; lane 3, grapevine virus D; lane 4, grapevine virus E; lane 5, grapevine virus F; lane 6, grapevine virus G; lane 7, grapevine virus H; lane 8, grapevine virus I; lane 9, grapevine virus J; lane 10, grapevine virus L; lane 11, grapevine virus M; lane 12, grapevine Pinot gris virus; lane 13, grapevine rupestris stem pitting-associated virus; lane 14, healthy grapevine; lane M, 1 Kb Plus DNA ladder marker. The expected amplicon size is 219 bp.



Given the success of the universal assay to amplify all the known grapevine vitiviruses, we investigated if this assay could also detect vitiviruses infecting other hosts. The universal assay generated a 219-bp product from mint infected with mint virus 2, which was confirmed by cloning and Sanger sequencing but failed to amplify a product from blueberry infected with blueberry green mosaic-associated virus (Fig. 2).

Figure 2. Analysis of different hosts infected by vitiviruses using the universal assay. Lane 1, blueberry infected by blueberry green mosaic-associated virus; lane 2, mint infected by mint virus 2; lane 3, grapevine infected by grapevine virus A; lane 4, healthy grapevine; lane M, 1 Kb Plus DNA Ladder marker.



Objective 4:

The universal RT-PCR assay was used to evaluate the occurrence of vitiviruses in the Davis Virus Collection (DVC) maintained by the University of California-Davis. The same plants were analyzed independently by individual assays for GVA to GVM. Grapevines testing positive by the universal assay tested positive by at least one of the individual assays, and all plants that tested negative by the universal assay were negative by all the individual assays. Overall, 185 of 385 (48%) DVC grapevines had single or mixed infections of GVA, GVB, GVD, GVE, and GVF. No GVG, GVH, GVI, GVJ, GVL, or GVM infected vines were detected.

Objective 5:

We had planned to evaluate the biological effects of GVG, H, I, J, L and M on the common grapevine indicators LN33 and Kober 5BB but we were not able to identify grapevines infected with the new vitiviruses that were not also co-infected with GVA and/or GVB. Therefore, while we are still hoping to evaluate these effects at some point, this work was not completed during this project.

Objective 6:

The novel detection tools developed for this proposal have been shared with private commercial diagnostic labs involved in the grape industry in the US, CDFA, and the National Clean Plant Network and will augment the production of certified propagation material and the effective control of vitiviruses infecting grapevine in California and beyond.

Summary

Until several years ago, nine different viruses were classified as vitiviruses (genus *Vitivirus*, family *Betaflexiviridae*) and known to infect grapevine: grapevine virus A (GVA), grapevine virus B (GVB), grapevine virus D (GVD), grapevine virus E (GVE), grapevine virus F (GVF),

grapevine virus G (GVG), grapevine virus H (GVH), grapevine virus I (GVI) and grapevine virus J (GVJ). Some of these vitiviruses are associated with rugose wood (RW) disease in grapevine and are vectored by mealybugs (family *Pseudococcidae*) and soft-scale insects (family *Coccidae*). However, the main route of transmission is by propagation using infected plant material. These vitiviruses are frequently detected in coinfection with members of the family *Closteroviridae*, i.e., grapevine leafroll-associated viruses 1, 2 and 3, resulting in synergistic interactions that can lead to lethal effects in several scion and rootstock combinations. Two new grapevine viruses were discovered by high throughput sequencing (HTS) during the last two years and have been proposed as members in the *Vitivirus* genus. These new viruses were tentatively named grapevine virus L (GVL) and grapevine virus M (GVM). In contrast with long known vitiviruses, i.e., GVA to GVF, the biological significance of GVG to GVM infections remains largely unknown, including effects on vine performance and mechanisms of transmission. In 2018, a limited survey was launched to determine the prevalence of GVG, H, I, J and L in California; all five viruses were detected with conventional RT-PCR across different grapevine populations. This project updated existing qPCR-based detection assays and in the case of the newer vitiviruses, designed qPCR assays to replace the conventional PCR-based assays. In addition, we developed a universal conventional RT-PCR assay that detects all 11 grapevine vitiviruses, which will increase the reliability and efficiency of vitivirus detection in grapevines. Although we were not able to evaluate the biological effects of the newer vitiviruses on LN33 and Kober 5BB, there isn't currently any evidence that they are associated with any disease. Specific biological studies are needed to definitively assess potential effects on vine performance but given the prevalence of vitivirus co-infections, this work will be difficult to complete. Finally, the qPCR-based assays developed in this project are available upon request to CA commercial diagnostic labs and public agencies to facilitate detection of all known vitiviruses and minimize their negative impact on the grapevine industry.

California Fruit Tree, Nut Tree, And Grapevine Improvement Advisory Board (IAB)

FINAL REPORT JUNE 2021

Project Title: Managing Fungal Trunk Diseases in Plant Nursery Stock. #20-1062-000-SA

Fiscal Year and Project Duration: First year of a 3-year project.

Project Leaders:

Dr. Philippe Rolshausen
Cooperative Extension Specialist
Dept. of Botany and Plant Sciences

Dr. Dario Cantu
Professor
Dept. of Viticulture and Enology,
UC Davis

Summary:

The overarching goal of this project is to improve the quality of plant nursery stock by decreasing the incidence of fungal pathogens causing wood diseases. We have established a partnership with several nurseries and collected and processed 320 commercial vines. Each vine received a wood health score based on the extend of wood necrosis and decay, from 3 sections in the cutting; above the graft union, below the graft union and root/rootstock. Disease diagnosis was performed from all three sections of the vine cutting using both culture-dependent and -independent strategies. Results from 90% of the samples using the culturing diagnosis approach indicated that *Pleurostoma*, *Cadophora* and *Phaeoacremonium* were the main pathogens, although other fungi (*Fusarium*) with higher incidence but with unknown aggressiveness to grapevine were also found. We are awaiting from sequencing data to complement the culture-based diagnosis and confirm the main pathogens involved. This information coupled with wood health data will provide clues with respect to potential infection routes.

Objectives:

- 1- Identify fungal trunk disease infection routes in nursery.
- 2- Profile trunk disease pathogens in nursery stock to improve accuracy of diagnostic tools.
- 3- Provide industry guidelines and training for best management practices and disease diagnostic.

Summary of Activities:

Objective 1- Identify fungal trunk disease infection routes in nursery.

Since the start of this project, we have established a partnership with several California nurseries and are still in the process of collecting plant materials. In order to minimize a 'plant effect' we sampled across all nurseries the same plant materials that include some of the most widely planted clones in California; Chardonnay Clone 4 x 1103P rootstock (80 vines per nursery) and Cabernet Sauvignon FPS 8 x 1103P rootstock (80 vines per nursery). Vines were either dormant or green depending on nursery availability.

In the laboratory at UC Riverside, vines cuttings were processed as follow; vines were washed to remove dirt, and bark was peeled-off with sterile knife. Each vine was then cut with sterile pruners in three sections; above the graft-union, below the graft union and the rootstock/root (**Figure 1**). Those sections were selected because they were described as the most prone for infection due to wounding during the propagation phase, which is the entry point for fungi causing trunk diseases (Gramaje and Armengol, 2011). Subsequently each section was surface sterilized by flaming, split in half with sterile knife, and wood health ratings were recorded ranging from 0 (= healthy wood, no necrotic lesion) to 3 (= canker; wood with extended wood necrosis with apparent dead cambium; **Figure 2**). Note that the wood cambium is the most vital tissue of plants because it regenerates the vascular system (phloem and xylem), and death of the cambium often leads to plant death. This information will give each vine cutting and each section a 0-9 and 0-3 wood health rating value respectively and will be correlated later to pathogen absence/presence and abundance.

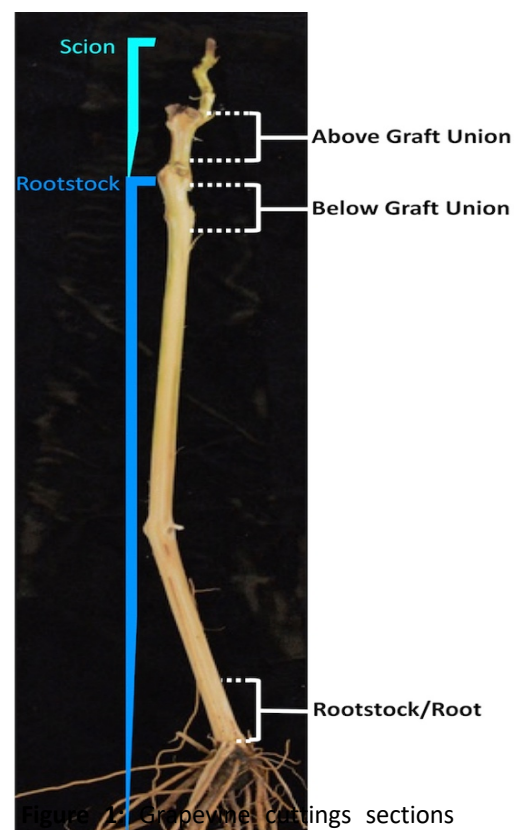


Figure 1. Grapevine cuttings sections used for culture-dependent and culture-independent analyses.

Wood Health Ratings

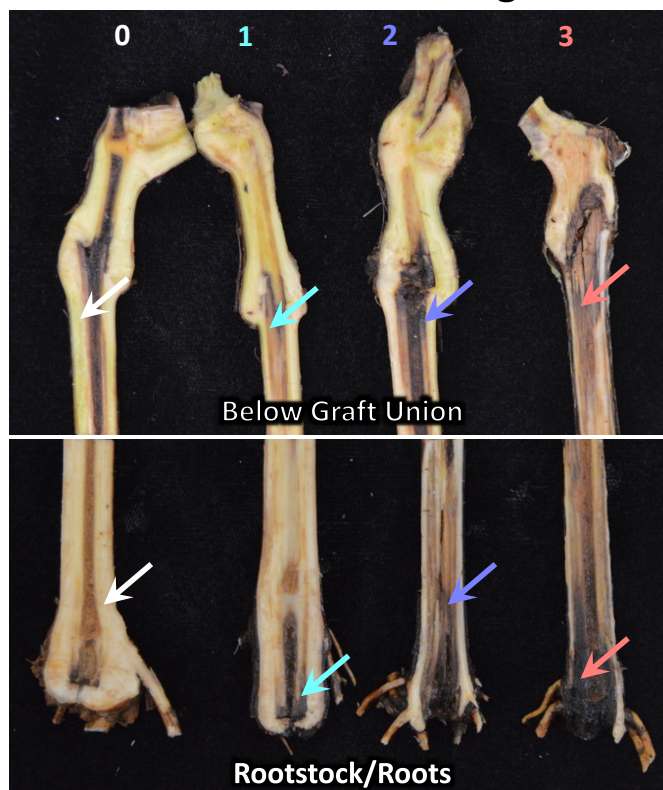


Figure 2: Rating system used to score plant nursery stock wood health. The two panels show wood health scores for two of the three wood cutting sections (see Figure 1); below the graft union and rootstock/root. 0 = healthy wood; 1 = <50% wood necrosis/decay; 2 = >50% wood necrosis/decay; 3 = canker with cambium death.

Results showed that Chardonnay Clone 4 x 1103P rootstock and Cabernet Sauvignon FPS 8 x 1103P rootstock displayed on average similar wood health ratings (about 3.9 on the 0-9 scale). However, not all plant sections displayed similar wood health ratings. Below the graft union showed above average scores indicating it has the most wood decay, while the scions showed the lowest ratings very little wood decay and this for both plant materials. Although, these values are subjective and do not translate into vine performance in vineyards, they are indicative of where pathogen presence are most likely to occur in the grafted vines, and help with identifying possible routes of infection.

After recording the wood health, one half portion of each section were frozen in liquid nitrogen, placed in falcon tube, stored in the freezer and shipped to UC Davis for culture-independent analyses using molecular protocols already developed by the Cantu laboratory (Morales-Cruz et al., 2018). About 70% were completely processed and send for sequencing. Results will be obtained shortly and will be presented in next year's report. Total DNA is being extracted from the remaining 30% of the samples.

The other half of each section were processed in the Rolshausen laboratory using standard microbiological techniques. Wood samples were surface sterilized in a 10% bleach bath for 1 min and rinsed in distilled water bath for 2min. Wood chips of ~3mm³ were cut from necrotic wood using a sterile knife and plated on potato dextrose agar culture medium amended with three antibiotics (ampicillin, neomycin and tetracycline at 1 mg/L each) to inhibit bacterial growth. After one week of incubation at room temperature, fungi were transferred to PDA plates to obtain a pure culture and fungal cultures were identified following a DNA extraction and PCR amplification of the ITS rDNA coupled with blasted in the NCBI database.

All samples were processed and diagnosis has been completed for 90% of the samples. Results showed that *Cadophora*, *Phaeoacremonium* and *Pleurostoma* were the three main known pathogens (Gramaje and Armengol, 2011; Raimondo et al., 2019) present in plant nursery stocks with an incidence ranging from 1.9% to 10% (Table 1). Several additional pathogens (*Ilyonectria*, *Diplodia*, *Neofusicoccum*, *Diaporthe*) were also found but at an incidence below 1% (see Obj.2). *Fusarium* was also highly prevalent in plants as previously reported in plant nurseries from Italy (Pintos et al., 2018), but the pathogenic status of this group to grapevine remains unclear. Interestingly, the biological control agent *Trichoderma* known for being antagonistic to many pathogens causing wood diseases in grapevine was also found at a high incidence in all plants.

Table 1: Incidence of the main beneficial (*Trichoderma*), pathogenic (*Cadophora*, *Pleurostoma*, *Phaeoacremonium*) and unknown status (*Fusarium*) in different wood cuttings areas (see Figure 1) for Chardonnay Clone 4 x 1103P rootstock and Cabernet Sauvignon FPS 8 x 1103P. (N= 160 vines)

Wood Cutting Areas	Fungal Incidence									
	Trichoderma		Fusarium		Cadophora		Phaeoacremonium		Pleurostoma	
	Chard	Cab	Chard	Cab	Chard	Cab	Chard	Cab	Chard	Cab
Above Graft Union	25.6%	31.9%	36.3%	16.9%	0.6%	2.5%	--	1.3%	5.6%	4.4%
Below Graft Union	26.9%	28.8%	35%	32.5%	0.6%	2.5%	0.6%	2.5%	4.4%	2.5%
Root-Rootstock	36.9%	43.1%	20%	23.1%	2.5%	3.1%	1.3%	0.6%	2.5%	--
Total	59.4%	68.1%	51.3%	45.6%	3.1%	6.3%	1.9%	3.8%	10%	6.9%

2- Profile trunk disease pathogens in nursery stock to improve accuracy of diagnostic tools.

Our results from 320 plants indicate that *Pleurostoma* was overall the main known pathogen in grape nursery stock, followed by *Cadophora* and *Phaeoacremonium* (Fig. 3). Additional DNA sequencing needs to be performed to determine the species name of those pathogens. Pathogenicity assays need to be performed on abundant taxa recovered from plants but with unknown aggressiveness to grapevine (i.e., *Fusarium*)

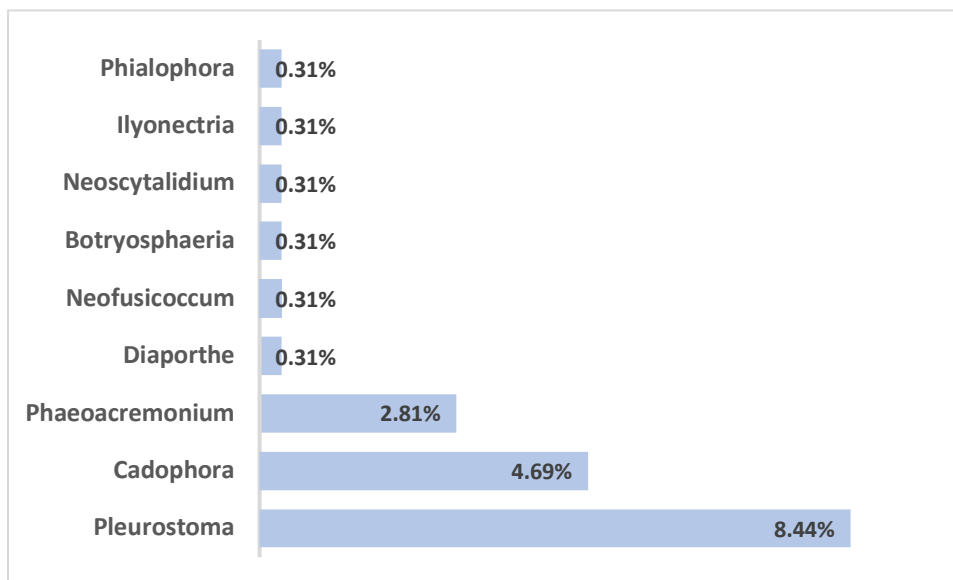


Figure 3: Incidence of the main known wood pathogens to grapevine in plant nursery stocks (n=320 plants).

3- Provide industry guidelines and training for best management practices and disease diagnostic.

Nothing to report for this objective at the moment.

References

- Gramaje D. and Armengol, J. 2011. Fungal trunk pathogens in the grapevine propagation process: potential inoculum sources, detection, identification, and management strategies. *Plant Disease*, 95: 1040-1055.
- Morales-Cruz A., Figueroa-Balderas R., Garcia J.F., Tran E., Rolshausen P.E., Baumgartner K. and Cantu D. 2018. Profiling grapevine trunk pathogens *in planta*: a case for community-targeted DNA metabarcoding. *BMC Microbiology*, 18:214.
- Pintos C., Redondo V., Costas D., Aguin O. and Mansilla P. 2018. Fungi associated with grapevine trunk diseases in nursery-produced *Vitis vinifera* plants. *Phytopathologia Mediterranea* 57:407-424.
- Raimondo M.L., Carlucci A., Cicca-Rone C., Sadallah A. and Lops F. 2019. Identification and pathogenicity of lignicolous fungi associated with grapevine trunk diseases in southern Italy. *Phytopathologia Mediterranea*, 58:639-662.